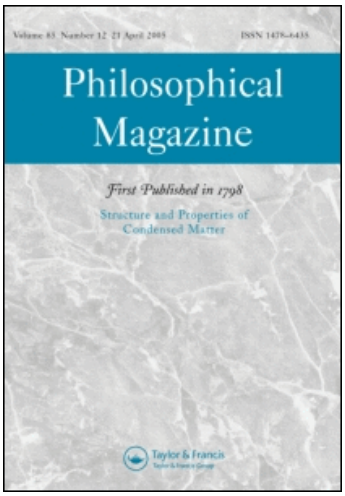

Philosophical Magazine
Publication details, including instructions for authors and subscription information:
http://www.informaworld.com/smpp/title~content=t713695589

Heterogeneous grain initiation in solidification

A. L. Greer [a]; T. E. Quested [a]
[a] Department of Materials Science & Metallurgy, University of Cambridge, Cambridge, CB2 3QZ, UK

Online Publication Date: 21 August 2006

To cite this Article Greer, A. L. and Quested, T. E.(2006)'Heterogeneous grain initiation in solidification',Philosophical Magazine,86:24,3665 — 3680
To link to this Article: DOI: 10.1080/14786430500198486
URL: http://dx.doi.org/10.1080/14786430500198486

Philosophical Magazine,
Vol. 86, No. 24, 21 August 2006, 3665–3680

Taylor & Francis
Taylor & Francis Group

Heterogeneous grain initiation in solidification

A. L. GREER* and T. E. QUESTED

Department of Materials Science & Metallurgy, University of Cambridge,
Pembroke Street, Cambridge CB2 3QZ, UK

(*Received 10 January 2005; in final form 18 May 2005*)

Grain refinement in casting of aluminium alloys can be quantitatively modelled by assuming that the barrier for grain initiation on an inoculant particle is that for free growth from the particle rather than for the initial formation of the solid. This leads to deterministic nucleation behaviour in which the number of grains is dependent on undercooling and not on time. Taking grain refinement of aluminium alloys as an example, the conditions for such *athermal nucleation* are analysed for a variety of nucleant particle shapes. The relevance for other cases, for example the action of ice-nucleating agents in living systems, is explored. In general, it is shown that for potent heterogeneous catalysis of solidification, the finite size of the nucleation sites renders classical nucleation theory inapplicable. The concept of nucleation in such a case is briefly discussed.

1. Introduction

In modelling of solidification, the nucleation of the solid phase presents the greatest challenge in making quantitative predictions based on independently determined parameters [1]. Not only are the relevant parameters often not well evaluated, but there are difficulties with the underlying theory. Probabilistic microstructural modelling to generate realistic grain structures requires the use of a nucleation law, and it is most commonly in the form of a dependence of the number of nuclei (n per unit volume) on undercooling (ΔT) [2]. For example, in the widely adopted approach of Thévoz *et al.* [3] the nucleation rate $\mathrm{d}n/\mathrm{d}\,\Delta T$ as a function of ΔT is taken to have a Gaussian form. Such a law gives a number of nuclei dependent on temperature but independent of time at a given temperature; this is in contrast to the time dependence expected from classical nucleation (whether homogeneous or heterogeneous). Time-independent nucleation has been termed *athermal* [4], and it occurs when sub-critical nuclei become critical, not by fluctuation past the critical size, but on cooling when the decreasing critical size sweeps past their own size.

As recently reviewed [5], athermal nucleation has a rôle in a very wide variety of transformations, but it is particularly relevant for the heterogeneous nucleation of solidification. This was first examined quantitatively by Turnbull. His work on dispersions of mercury droplets, used to measure the rate of homogeneous

*Corresponding author. Email: alg13@cam.ac.uk

Philosophical Magazine
ISSN 1478–6435 print/ISSN 1478–6443 online © 2006 Taylor & Francis
http://www.tandf.co.uk/journals
DOI: 10.1080/14786430500198486

nucleation under isothermal conditions at large ΔT [6], is well known. In some experiments, however, he found that the droplets could not be undercooled more than 2–4 K [7]; in these cases, the fraction of droplets solidified was dependent on ΔT but not on time. Turnbull suggested that the droplets were contaminated and that surface patches acted as nucleants. A thin coating of the solid phase on a patch becomes a transformation nucleus only when, on cooling, the critical nucleation radius r^* becomes equal to, and then less than, the radius of the patch. He then used the measured fraction of solidified droplets as a function of ΔT to derive the size distribution of the patches.

More recently, it has been proposed that athermal nucleation of a similar kind can explain the performance of inoculants in grain-refining of commercial aluminium alloys. Inoculation with, for example, an Al–Ti–B master alloy introduces stable TiB_2 particles to the melt and these are the dominant nucleation sites. The particles are hexagonal prisms and nucleation of solid aluminium is on their flat {0001} faces [8]. In the *free-growth* model of Greer *et al.* [9], the hexagonal faces are approximated as circles, and it is proposed that grain initiation on a particle occurs not when the solid first appears on its surface, but when the solid, growing outward as cooling continues, passes the critical hemispherical shape at which the radius of curvature of its interface with the melt is minimum. This is equivalent to Turnbull's condition that a transformation nucleus is formed when r^* is equal to the radius r_P of the nucleant surface on the particle. Greer *et al.* inverted the calculation of Turnbull: by measuring the distribution of r_P, they calculated the distribution of ΔT at which grains would nucleate and, using a model balancing latent heat release with external heat extraction (based on earlier work [10]), predicted grain size as a function of refiner addition level, alloy solute content and cooling rate. Unusually, the model does appear capable of quantitative prediction of a nucleation phenomenon without adjustable parameters.

Analyses of nucleation on particles have typically been based on the work of Fletcher [11–13], who examined the rôles of particle size and shape. These analyses are based, however, on classical heterogeneous nucleation involving thermal activation over an energy barrier. In contrast, the approaches of Turnbull [7] and of Greer *et al.* [9] offer a justification for a deterministic law for athermal nucleation, in which each nucleant site or particle has a critical ΔT, inversely proportional to its linear dimension, at which it becomes a transformation nucleus. In the present work, we focus on grain refinement of aluminium alloys (a process which has been extensively reviewed [14–17]) as an example of nucleation catalysis in solidification. Grain nucleation is clearly heterogeneous, on added nucleant particles, and it occurs at very small undercooling, typically <0.2 K. It will be shown that the limited size of the nucleant particles makes classical nucleation theory inapplicable in such a case. The work of formation of solid on nucleant particles is calculated for various particle shapes. The solid is dormant until the critical undercooling for free growth of a grain is reached. The influence of the dormant solid is analysed, as is the competition between stochastic thermal nucleation and deterministic athermal nucleation. Other examples are identified in which athermal heterogeneous nucleation of solidification is likely to be dominant.

2. Grain initiation on a circular particle face

2.1. *Grain refinement of aluminium by Al–Ti–B*

As noted earlier, a common inoculant for aluminium alloys is the Al–Ti–B system in which the nucleant particles are hexagonal prisms of TiB_2. We have taken this as the basis for our analysis; other cases are considered in section 4. The nucleant faces of the TiB_2 particles are {0001}, in the form of plane hexagons; these are approximated as plane circles (figure 1a). It is known that the TiB_2 particles are very powerful nucleants for α-Al, and it has been suggested that the solid may even start to form on the particles above the alloy liquidus temperature, stabilized by adsorption. The rôle of adsorption in heterogeneous nucleation of solidification has been briefly reviewed elsewhere [5]. For the particular case of inoculation of aluminium, the adsorption-based *hypernucleation* model of Jones [18, 19] provides a basis for selection of potential inoculants, microscopical observations provide some evidence for an adsorbed layer [8], and the success of modelling based on the free-growth criterion [9] suggests that the onset of free growth rather than the initial appearance of solid is the critical barrier for initiation of a grain.

In the following we consider the formation of solid on one of the {0001} faces of a disc-shaped particle. Whether by adsorption or by classical heterogeneous

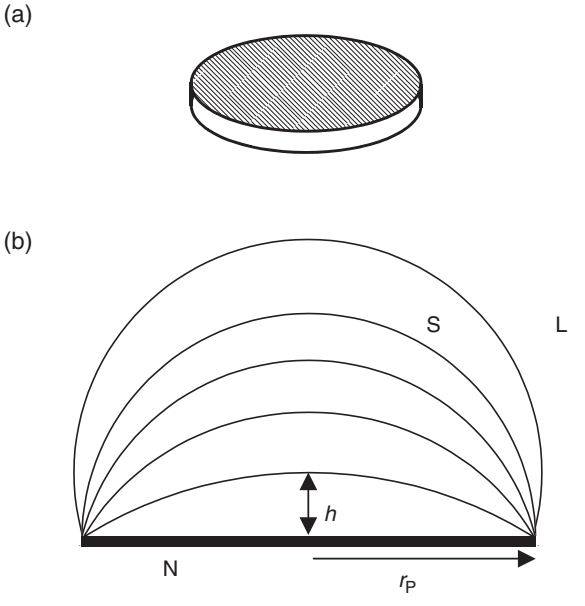

Figure 1. Hexagonal TiB_2 particles in Al–Ti–B master alloys can be approximated as circular discs (a). Nucleation of α-Al occurs on the circular {0001} faces only. Growth (b) of the nucleated solid S into the liquid L and outward from the face of the particle N involves an increase in curvature of the liquid/solid interface as permitted by an increase in undercooling. The curvature is maximum when the liquid/solid interface is hemispherical. Free growth beyond that point during cooling constitutes athermal nucleation.

nucleation with a very low contact angle, a thin layer of solid coats the circular face. Subsequent growth of the solid can only be outwards as microscopical evidence suggests that α-Al avoids contact with the prismatic faces of the TiB_2 particles. The solid takes the form of a spherical cap and its growth can be represented by its height h (figure 1b). As h increases, the liquid/solid interface becomes more curved and growth must stop when the radius of curvature of the interface r_{LS} has decreased to equal r^*, the critical nucleation radius for the ambient undercooling ΔT. For small ΔT, it is readily derived [20] that

$$r^* = \frac{2\gamma_{LS}}{\Delta S_V \Delta T} \tag{1}$$

where γ_{LS} is the free energy (per unit area) of the liquid/solid interface and ΔS_V is the entropy of fusion per unit volume. The solid is dormant, as it is not yet a nucleus for solidification of the entire liquid. As the undercooling is increased, r^* decreases and the solid, for which $r_{LS} = r^*$, can grow. When r^* has decreased to equal r_P the solid forms a hemisphere, r_{LS} has its minimum value, and the solid can subsequently grow freely, forming a grain and ultimately permitting solidification of the entire liquid. The critical undercooling for the onset of this free growth, from equation (1), is given by

$$\Delta T_{fg} = \frac{2\gamma_{LS}}{\Delta S_V r_P}. \tag{2}$$

The onset of free growth on successively smaller particles as ΔT is increased constitutes athermal nucleation. In modelling of the grain refinement of aluminium alloys [9], it has been assumed that a grain is initiated on a nucleant particle at exactly ΔT_{fg}, i.e. that the behaviour is completely deterministic. However, it is conceivable that the onset of free growth on a particle could be preceded by thermal activation of nucleation over an energy barrier; if that were so, grain initiation could be a stochastic process. This possibility is now examined.

2.2. *Work of formation of the solid cap*

As analysed elsewhere [5], the work of formation of a spherical cap of solid of height h covering the circular face of a nucleant particle of radius r_P is

$$W_{cap} = \gamma_{LS}\pi h^2 - \Delta S_V \Delta T\left(\frac{\pi h^3}{6} + \frac{\pi r_P^2 h}{2}\right). \tag{3}$$

The reference point for energy (i.e. when $W_{cap} = 0$) has been taken to be an infinitesimally thin layer of solid coating the circular face of the particle. For this reason, the interfacial-energy contribution to the work of formation (i.e. the first term on the right-hand side of equation (3)) involves only changes in the area of the liquid/solid interface. The free-energy change associated with solidification itself scales with the volume of the spherical cap and is given by the second term on the right-hand side of equation (3).

The universal form of W_{cap} is best presented in terms of dimensionless quantities. A given shape of solid cap should then correspond to a given dimensionless undercooling. The dimensionless cap height is taken to be h/r_P. The dimensionless

undercooling is obtained by normalizing with respect to the free-growth undercooling (equation (2)). The onset of free growth (i.e. athermal nucleation) is when the dimensionless undercooling $\Delta T/\Delta T_{fg} = 1$. A dimensionless work of formation is obtained by normalizing with respect to $W^*_{\Delta T_{fg}}$, the critical work for homogeneous nucleation at the free-growth undercooling ΔT_{fg}:

$$W^*_{\Delta T_{fg}} = \frac{16\pi\gamma_{LS}^3}{3\Delta S_V^2 \Delta T_{fg}^2} = \frac{4\pi\gamma_{LS} r_P^2}{3}. \tag{4}$$

Expressing equation (3) in terms of these dimensionless quantities gives

$$\frac{W_{cap}}{W^*_{\Delta T_{fg}}} = -\frac{1}{4}\left(\frac{\Delta T}{\Delta T_{fg}}\right)\left(\frac{h}{r_P}\right)^3 + \frac{3}{4}\left(\frac{h}{r_P}\right)^2 - \frac{3}{4}\frac{\Delta T}{\Delta T_{fg}}\frac{h}{r_P}. \tag{5}$$

The form of equation (5) is plotted in figure 2 for five values of dimensionless undercooling. For $\Delta T < \Delta T_{fg}$, the work of cap formation has a minimum followed by a maximum as h/r_P is increased. These extrema correspond to equilibrium across the liquid–solid interface when its radius of curvature has the critical value r^* given by equation (1), expressed in dimensionless terms as

$$\frac{r^*}{r_P} = \frac{\Delta T_{fg}}{\Delta T}. \tag{6}$$

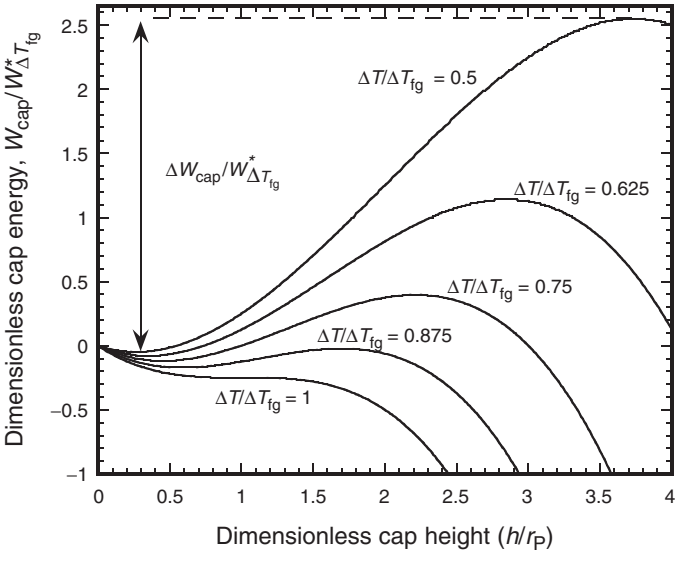

Figure 2. Dimensionless work of formation ($W_{cap}/W^*_{\Delta T_{fg}}$) of solid cap on a circular nucleant area as a function of dimensionless cap height (h/r_P) for selected values of dimensionless undercooling ($\Delta T/\Delta T_{fg}$) (equation (5)). The minima (maxima) in these energy curves represent metastable (unstable) equilibrium configurations.

The corresponding solid caps are the two portions of a sphere of equilibrium curvature r^* formed when the sphere is cut by a plane, such that the circle of intersection has a radius equal to r_P. The smaller portion corresponds to the minimum in the curves in figure 2 and is the shape adopted in metastable equilibrium (figure 3, inset (a)); the larger portion corresponds to the maximum and represents an unstable equilibrium (figure 3, inset (b)).

As an example, the curve for $\Delta T/\Delta T_{fg} = 0.5$ from figure 2 is reproduced in figure 3, together with a plot of r_{LS}. Between the two extrema shown, $r_{LS} < r^*$. The variation of the work of cap formation with cap height clearly indicates the energy barrier for nucleation, which exists when $\Delta T/\Delta T_{fg} < 1$. In figure 2 the energies on the different curves can be directly compared as the normalization is with respect to the fixed quantity $W^*_{\Delta T_{fg}}$. As the undercooling is increased, the two extrema converge and the barrier decreases. At $\Delta T/\Delta T_{fg} = 1$, the work of formation as a function of cap height no longer has extrema, but only a stationary point at which*1for0.sed-8.2.fort1CTfaeprzi00952.roug-8.2twoTJ-17.fordirz.heightrespect to the fied uation with respect to the fied uantity*

2.3. *The competition between thermal and athermal nucleation*

The initial, infinitesimally thin, coating of solid on the particle face grows naturally to the metastable and dormant condition corresponding to the minima in the curves shown in figure 2. From that condition, the critical work of thermal nucleation ΔW_{cap} is the difference in energy between the two extrema (figure 3), which can be expressed as

$$\frac{\Delta W_{\mathrm{cap}}}{W^*_{\Delta T_{\mathrm{fg}}}} = \left[\left(\frac{\Delta T_{\mathrm{fg}}}{\Delta T}\right)^2 - 1\right]\sqrt{1 - \left(\frac{\Delta T}{\Delta T_{\mathrm{fg}}}\right)^2}. \tag{7}$$

The ratio $\Delta W_{\mathrm{cap}}/W^*_{\Delta T_{\mathrm{fg}}}$ tends to infinity (or 0) as $\Delta T/\Delta T_{\mathrm{fg}}$ tends to 0 (or 1). The critical work for nucleation (equation (7)) is plotted (on a logarithmic scale) as a function of undercooling in figure 4, and shows a sharp transition. For small $\Delta T/\Delta T_{\mathrm{fg}}$, the dimensionless work $\Delta W_{\mathrm{cap}}/W^*_{\Delta T_{\mathrm{fg}}} \gg 1$, while for large $\Delta T/\Delta T_{\mathrm{fg}}$ the work $\Delta W_{\mathrm{cap}}/W^*_{\Delta T_{\mathrm{fg}}} \ll 1$. The likelihood of thermal activation over this energy barrier depends on the ratio of the barrier height ΔW_{cap} to the thermal energy $k_{\mathrm{B}}T$ (where k_{B} is Boltzmann's constant and T is the temperature). Thermal activation is expected to become significant when $\Delta W_{\mathrm{cap}} \leq k_{\mathrm{B}}T$. For thermally activated nucleation to occur significantly before the onset of free growth, the dimensionless work must meet the condition:

$$\frac{\Delta W_{\mathrm{cap}}}{W^*_{\Delta T_{\mathrm{fg}}}} \leq \frac{3k_{\mathrm{B}}T}{4\pi\gamma_{\mathrm{LS}}r_{\mathrm{P}}^2} \tag{8}$$

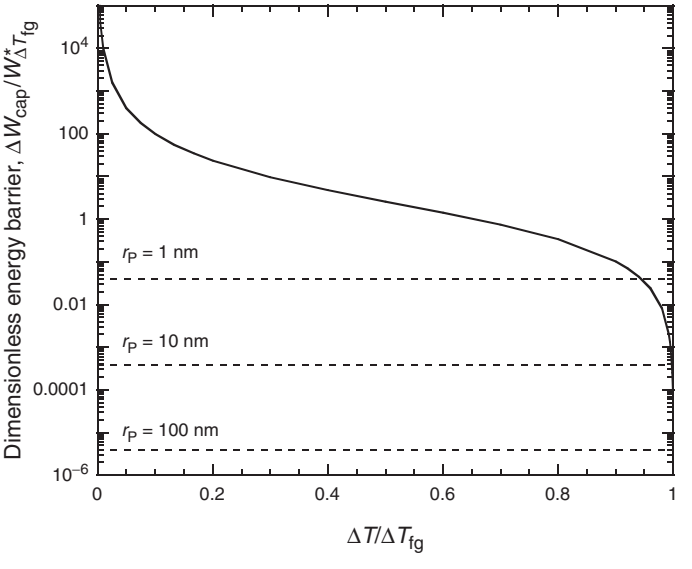

Figure 4. The dimensionless critical work of nucleation ($\Delta W_{\mathrm{cap}}/W^*_{\Delta T_{\mathrm{fg}}}$) as a function of dimensionless undercooling ($\Delta T/\Delta T_{\mathrm{fg}}$) (equation (7)) for a solid cap forming on a circular nucleant area. The dashed lines indicate values (dependent on particle radius r_{P}) of the critical work below which, during cooling, thermal activation of nucleation is likely to precede the onset of free growth (equation (8)). Calculations are for aluminium alloys.

where $W^*_{\Delta T_{fg}}$ is taken from equation (4). Clearly, this condition depends on the particle size and on γ_{LS}. For the inoculation of aluminium, we can take T to be the melting point of the metal (933.5 K) and $\gamma_{LS} = 158\,\mathrm{mJ\,m^{-2}}$ [21], as used in earlier work [9]. The values of dimensionless work from equation (8) are plotted on figure 4 for selected values of particle radius. When the curve falls below a given horizontal, thermally activated nucleation is likely to anticipate free growth. Figure 4 shows that such thermal activation is significant only at dimensionless undercoolings $\Delta T/\Delta T_{fg}$ approaching one. It is more likely for smaller particles, but even for the smallest particle considered, with $r_P = 1$ nm, it would be significant only for $\Delta T/\Delta T_{fg} > 0.95$. For a typical Al–Ti–B master alloy added to an aluminium melt, the TiB_2 particles on which grain nucleation actually occurs have nucleant faces at least 1.5 μm in radius [9]. For such a radius, thermal activation is significant only for $(1 - \Delta T/\Delta T_{fg}) < 10^{-8}$. The assumption in earlier work [9] that grain initiation would be purely athermal, following the condition in equation (2), is shown in figure 4 to be fully justified: for micrometre-sized particles, the chances of nucleation being thermally activated in advance of the onset of free growth are indeed negligible. Figure 5 summarizes the regimes of behaviour, showing when initial solid formation or alternatively free-growth onset is controlling (i.e. has the larger critical undercooling), and when thermal activation of nucleation is possible.

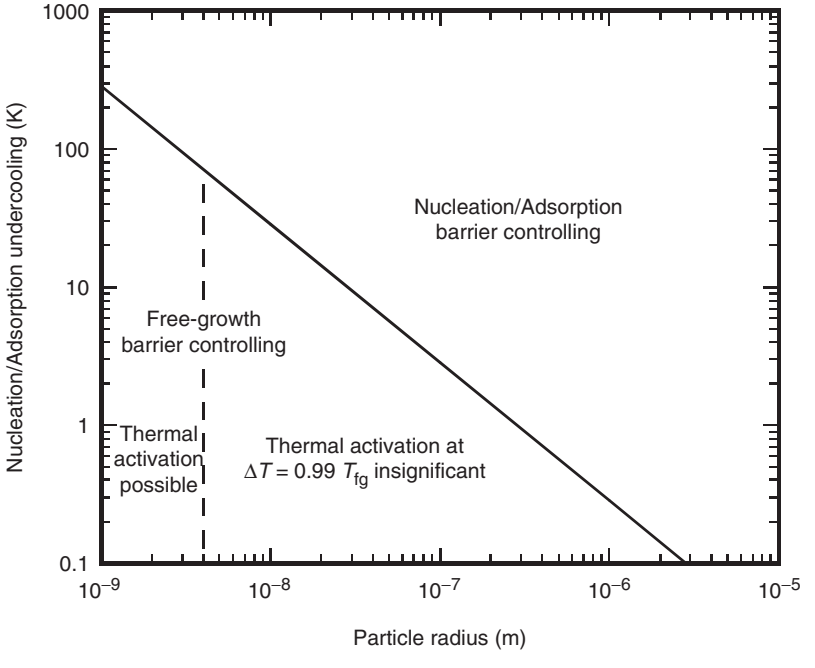

Figure 5. The initiation of an aluminium grain may be controlled by the initial formation of solid (by nucleation or adsorption on the nucleant particle) or by the onset of free growth. The regimes (of the critical undercooling for nucleation or adsorption, and of particle radius) in which one or other process is controlling are shown. The particle radius for which the free-growth barrier can be overcome by thermal activation is also indicated.

2.4. *Effects of dormant solid*

The free-growth model [9, 22] already used extensively in analysing the grain refinement of aluminium alloys is based on the assumption of a spatially isothermal melt. In many cases this is a reasonable assumption given that the thermal diffusion length can greatly exceed grain diameters. The numerical model computes the balance between external heat extraction and the production of latent heat as grains grow; when the latter dominates, the consequent reheating of the melt (*recalescence*) stifles any further athermal nucleation, determining the number of nucleated grains and thereby the grain size. The fraction solidified at the onset of recalescence is, under typical solidification conditions, small [9], of the order of 10^{-4}. The analysis in section 2.2 shows that before the onset of free growth on a given particle, there is a spherical cap of dormant solid. In the modelling undertaken and reported so far, this dormant solid has been ignored; that is, the volume of solid associated with each nucleant particle has been taken to be zero until the onset of free growth. Given that the fraction solidified at the onset of recalescence is so low, it is reasonable to consider whether the existence of dormant solid could significantly change the thermal balance.

The model used in earlier work [9] has been adapted to include dormant solid, assuming that on each nucleant particle the solid adopts its metastable equilibrium configuration. Partitioning of alloy solutes could restrict the growth of the solid; such effects are reviewed in general in [23], and the relevance for the onset of free growth is assessed in [5]. With any restriction of solid growth by partitioning, grain initiation would still be deterministic but delayed and there would be a smaller volume of dormant solid than calculated here. Thus the old model ignoring dormant solid and the new adaptation provide (respectively) lower and upper bound estimates of the effect of dormant solid on recalescence. The two models are compared in figure 6. The inclusion of dormant solid does detectably increase the solidified fraction during the early stages of solidification, and the associated latent heat release does decrease the undercooling. As solidification progresses, however, the effect of the dormant solid becomes negligible. Under typical conditions for casting of inoculated aluminium alloys, the inclusion of dormant solid in the calculations has an insignificant effect on the predicted maximum undercooling and therefore on grain size. Thus earlier calculations [9] are not invalidated by the neglect of dormant solid.

3. Shape of nucleant

The analyses in section 2 are for a plane circular nucleant area, which is a good approximation to the actual nucleant faces on TiB_2 particles. As noted more explicitly elsewhere [5], the analyses would apply equally for circular nucleant patches (of the kind considered by Turnbull [7]) on a more extensive substrate. If the nucleant area (face of a particle, or a patch) were concave or convex the curves in figure 2 would effectively start, respectively, at a negative or positive value of h, but otherwise the analysis is little affected [5]. Growth from a concave surface is very close to the case, originally analysed by Turnbull [24], of solidification triggered by residual solid in cavities, if the outer surface of the substrate is not wetted by the solid. Turnbull noted that the extent to which a melt can be undercooled may increase strongly with

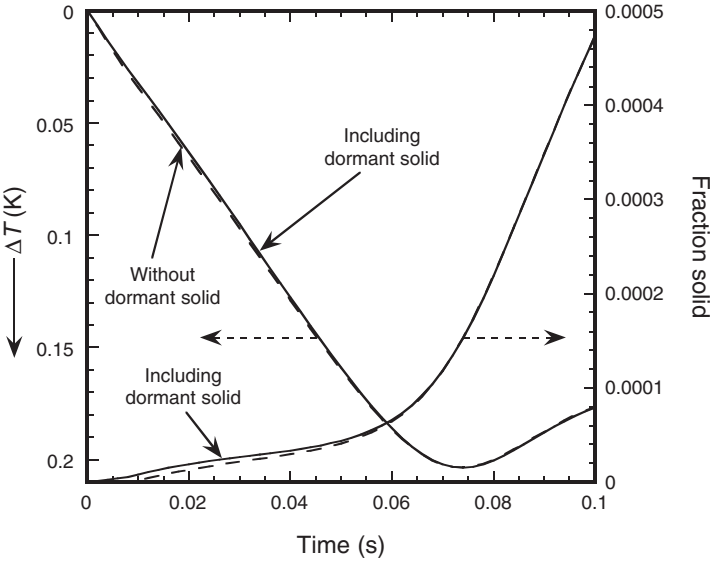

Figure 6. Comparison of predictions from two versions of the isothermal-melt model, in which the effect of dormant solid has been either included or omitted (solid and dashed lines respectively). Volume fraction of solid and undercooling are plotted for a typical aluminium alloy under standard casting conditions: cooling rate $= 3.5\,\mathrm{K\,s^{-1}}$, $Q = 2.2\,\mathrm{K}$, addition level of Al–5Ti–1B refiner $= 1$ ppt.

the degree to which it was previously superheated above its liquidus temperature T_{liq}. This arises from the survival of the solid above T_{liq} in cavities (in a mould wall or other substrate). The greater the superheat, the fewer nuclei survive, and the smaller the mouth of the cavities in which they survive. Subsequently, the ΔT at which the surviving nuclei become active is inversely proportional to the radius of the cavity mouth. The cases of cylindrical and conical cavities have been analysed [24].

A special case of a convex nucleant of limited size is that of a spherical nucleant particle. As before we assume that the particle is coated with a thin layer of solid, although on a sphere (as for any convex surface) the formation of such a coating is hindered by the Gibbs–Thomson effect. The solid can grow outwards as a sphere of radius r, centred on the particle of radius r_{P}. Taking the reference state to be, as before, that of the particle with an infinitesimally thin coating, the work of formation of the spherical shell of solid is

$$\frac{W_{\mathrm{shell}}}{W^{*}_{\Delta T_{\mathrm{fg}}}} = 3\left(\frac{r}{r_{\mathrm{P}}}\right)^{2} - 2\left(\frac{\Delta T}{\Delta T_{\mathrm{fg}}}\right)\left(\frac{r}{r_{\mathrm{P}}}\right)^{3} + 2\left(\frac{\Delta T}{\Delta T_{\mathrm{fg}}}\right) - 3 \tag{9}$$

where normalization is performed as before, with $W^{*}_{\Delta T_{\mathrm{fg}}}$ still given by equation (4). The variation of the work of formation with radius is shown in figure 7 for selected values of undercooling. The curves do not show a minimum, so in this case the configuration of the dormant solid is just the infinitesimal coating on the nucleant particle. As in the previous case of a plane circular nucleant face

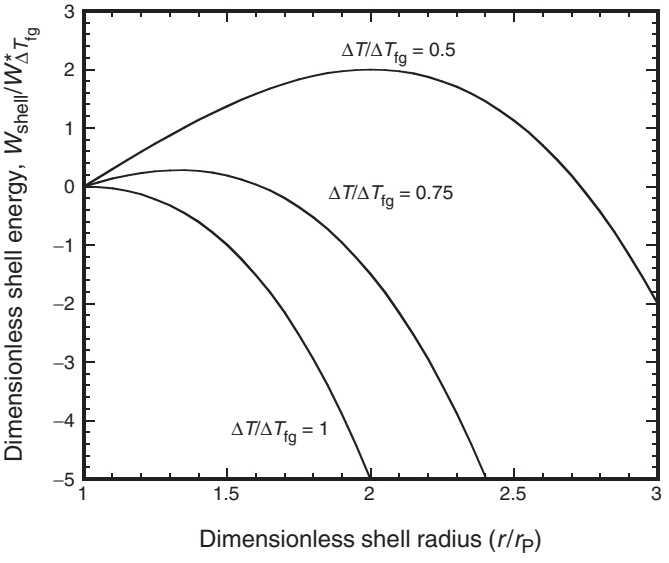

Figure 7. Dimensionless work of formation ($W_{shell}/W^*_{\Delta T_{fg}}$) of a solid shell on a spherical nucleant particle as a function of dimensionless outer shell radius (r/r_P) for selected values of dimensionless undercooling ($\Delta T/\Delta T_{fg}$) (equation (9)). The maxima in these energy curves represent an unstable equilibrium.

(equation (5), figure 2), there is an energy barrier for thermal nucleation which decreases as the dimensionless undercooling $\Delta T/\Delta T_{fg}$ increases towards one. The onset of free growth is when $\Delta T/\Delta T_{fg} = 1$. The energy barrier is given by

$$\frac{\Delta W_{shell}}{W^*_{\Delta T_{fg}}} = \left(\frac{\Delta T_{fg}}{\Delta T}\right)^2 + 2\left(\frac{\Delta T}{\Delta T_{fg}}\right) - 3 \tag{10}$$

and is shown in figure 8. As for a plane circular nucleant (figure 4), this shows that thermal nucleation is unlikely to be significant before the onset of free growth, for particles of typical size. As in figure 4, the horizontal dashed lines indicate energy barriers for different particle sizes (from equation (8), but with ΔW_{shell} substituted for ΔW_{cap}).

Apart from Al–Ti–B, the most common system used for inoculation of aluminium alloys is Al–Ti–C, which introduces TiC nucleant particles to the melt. Among the relative merits and demerits of the two systems [25] is the fact that the Al–Ti–C system appears to need a larger undercooling for grain initiation. Since the TiC particles are significantly smaller than their TiB_2 counterparts [26], this observation appears to be in accord with the free-growth model. This model is also supported by microstructural observations showing that grains are initiated only on the larger TiC particles [27]. In general, numerical modelling to predict grain size, of the kind used for Al–Ti–B refiners [9], works well also for Al–Ti–C refiners [26], although a fully quantitative measurement of the particle size distribution is thwarted by particle agglomeration. The nucleant phase TiC is cubic and the particles are in the form of an octahedron with {111} faces. Since the α-Al and the TiC

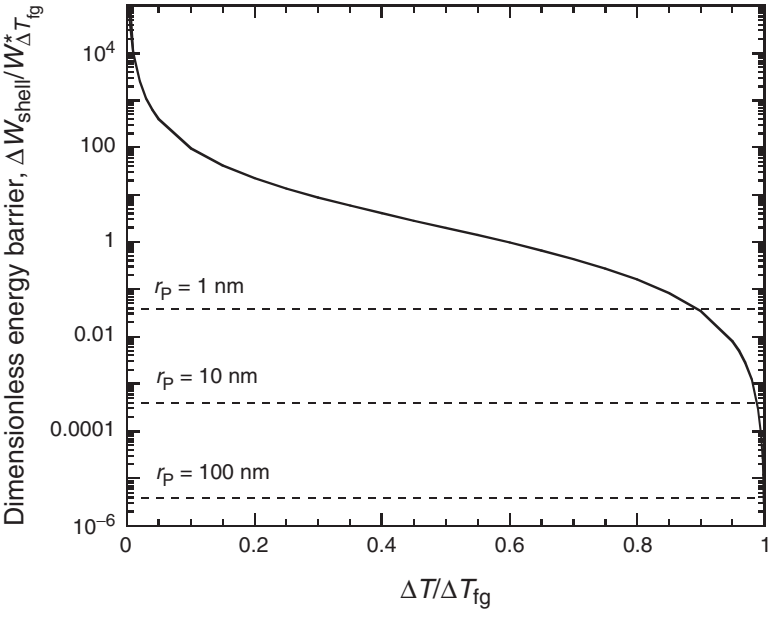

Figure 8. The dimensionless critical work of nucleation ($\Delta W_{shell}/W^*_{\Delta T_{fg}}$) as a function of dimensionless undercooling ($\Delta T/\Delta T_{fg}$) (equation (10)) for a solid shell forming on a spherical nucleant. The dashed lines indicate values (dependent on particle radius r_P) of the critical work below which, during cooling, thermal activation of nucleation is likely to precede the onset of free growth (equation (8) but with ΔW_{shell} instead of ΔW_{cap}). Calculations are for aluminium alloys.

have a cube–cube orientation relationship, it is assumed that all the {111} faces can be equally active. Grain initiation on such a particle involves processes already considered for plane circular and spherical nucleant areas. The plane faces on the TiC particle facilitate the initial formation of solid without inhibition by the Gibbs–Thomson effect. On cooling, the solid on each face can thicken with a liquid/solid interface of uniformly increasing curvature. When the interface has a curvature approximately of a sphere co-centric with the octahedron and touching the mid-points of its edges, the liquid/solid interfaces formed on each {111} face start to become continuous, and subsequent growth of the solid reduces the curvature of its interface with the liquid. This configuration marks the onset of free growth, analogous to the hemisphere on a plane circular nucleant. In similar ways the critical configurations can be determined for other nucleant particle shapes.

4. Finite size of nucleants in other cases

The solidification of inoculated aluminium alloys offers a clear example of nucleation effectively limited by the finite size of the heterogeneous nucleant areas. Other examples are widespread, extending beyond the solidification of metallic alloys. A case which has been particularly thoroughly studied is that of the nucleation

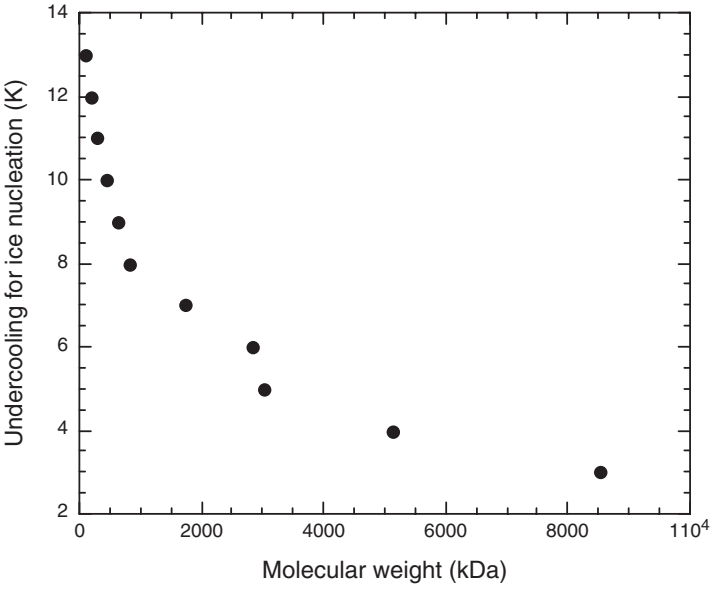

Figure 9. The measured dependence of the critical undercooling for ice nucleation on the molecular weight of the ice-nucleating agent for a particular bacterial strain *Pseudomonas syringae*. (Data from [32]).

of gas bubbles in a supersaturated liquid. As reviewed by Jones *et al*. [28], several types of nucleation can be distinguished. Of these, the mechanism (Type III nucleation in the classification of Jones *et al*. [28]) operating in a typical carbonated drink (for example champagne [29, 30]) is closely analogous to the free-growth model (figure 1b). Pre-existing bubbles in cavities (typically hollow cellulose fibres of well defined internal radius) are active nuclei as long as the supersaturation exceeds that corresponding to a critical nucleation radius r^* less than that of the fibre radius. As the drink becomes decarbonated, r^* increases and bubble nucleation can occur only at coarser and coarser fibres. Quite different from the solidification case, a nucleated bubble, after some growth, breaks free from the nucleant site and rises to the surface, enabling the nucleant site to act as the source of a stream of bubbles. Quantitative analysis of bubble size in the stream permits derivation of the nucleant size [29, 30].

Finite-size effects are also particularly evident in the operation of ice-nucleating agents (INAs) in living systems [31]. Systems as diverse as bacteria, insects and amphibians may use INAs to induce ice formation at smaller undercoolings than would otherwise be the case. Bacteria use INAs to promote frost damage from which they benefit. Insects and amphibians use INAs to promote ice formation in their extracellular fluid, thus forestalling ice formation within their cells, which would be fatal. The INAs are proteins specifically adapted to form a nucleant surface for ice. A typical folded protein has a linear dimension of no more than $\approx$10 nm, however, suggesting that size effects are important. The barrier to free growth is dominant. Figure 9 shows the measured correlation, for a particular bacterial strain [32], between the critical undercooling for ice nucleation and the molecular weight of the INA.

Behaviour of this kind has so far been interpreted in terms of classical nucleation on finite-sized particles of various shapes [13, 33]; it remains to be seen whether an analysis based on the free-growth barrier can provide a better quantitative fit to the data. Such an analysis clearly needs to take the shape of the INA into account.

5. Discussion

The initial formation of a new phase on a heterogeneous substrate is not sufficient to nucleate an overall transformation to the new phase if the substrate is too small. This finite-size effect has been analysed for plane circular nucleant areas and for spherical nuclei. In these geometrically simple cases the restriction of free growth from the initially formed solid occurs when the characteristic radius of the nucleant r_P is less than the critical radius r^* for nucleation under the given conditions. In the case of interest in the present work, the inoculation of metallic melts with potent nucleants, grain initiation is controlled by the onset of free growth at a critical undercooling particular to each nucleant particle and inversely proportional to r_P. It is important to note, however, that the first solid must form on the nucleant particles at an undercooling smaller than ΔT_{fg}. Regardless of whether the first solid forms by any type of heterogeneous nucleation or by adsorption or wetting, the condition for the free-growth onset to be dominant is met only when the nucleants are potent. This depends not only on the intrinsic potency of the particles, but also on their stability in the melt and potentially on the poisoning action of certain solutes [14–17]. And there are yet other factors which can have an important influence on grain refinement in practice, including cooling rate, growth restriction by solutes, particle agglomeration and settling.

For potent grain initiation the nucleant particles must be sufficiently large, and in practice r_P is of the order of 1 μm. For such a size, as shown in figures 4 and 8 for plane circular nucleant areas and for spherical nuclei, there is a negligible chance of athermal nucleation being pre-empted at smaller undercooling by the stochastic process of thermal nucleation. Thus for practical inoculation of aluminium alloys, the initiation of grains is completely deterministic and governed by the undercooling. This justifies the use of an athermal nucleation law as commonly used in modelling of solidification.

When the nucleant is planar, the metastable equilibrium configuration of the solid (represented by the energy minimum in, for example, figure 2) is dependent on the undercooling. The metastable equilibrium height h of the solid cap increases with undercooling, and as analysed elsewhere [5], the rate of increase dh/dt diverges to infinity as $\Delta T/\Delta T_{fg}$ approaches one. It impossible for the dormant cap to maintain the metastable configuration, as dh/dt may be limited by any of several factors: interfacial kinetics, transport of heat and transport of solute. For solidification of a typical alloy, the most important of these is the transport of solute. It has been shown that even for commercial-purity aluminium, growth restriction by solute is likely to be significant, leading to some kinetic inhibition of the onset of free growth [5]. Grain initiation would still be deterministic rather than stochastic. Kinetic inhibition of free growth onset does not arise for a spherical nucleant (section 3) because the dormant solid has an unchanging configuration.

Nucleation usually involves activation over an energy barrier and it is of interest to consider whether the term can correctly be applied to processes, such as the onset of free growth. In much of the present article the more general term grain *initiation* has been used. The initial formation of solid may involve true heterogeneous nucleation, but at the small undercoolings which are relevant, it is likely that classical nucleation cannot apply [5]. If the initial formation of solid is by adsorption, then there is no nucleation stage. Whatever the mechanism by which the initial solid is formed, it does not act as a transformation nucleus [4] until the free-growth undercooling is reached. Free growth of the grain occurs, not because any energy barrier has been surmounted, but because the barrier has disappeared as a result of increasing undercooling. Given that this process has been termed *athermal nucleation* [4], and that effectively it constitutes nucleation of the grain, it is reasonable to consider it to be a type of nucleation.

6. Conclusions

Inoculation to grain-refine aluminium alloys provides an example of the use of potent nucleant particles. In such a case, solid can form on a particle (by heterogeneous nucleation or by adsorption or wetting) at an undercooling smaller than that required for the onset of free growth, which constitutes the effective nucleation of a grain on the particle. This is an effect of the limited size of the particles. The larger the particle, the more potent it is as a nucleant. The energetics of the onset of free growth have been analysed in detail for a nucleant in the form of a plane circular area (a reasonable approximation to the {0001} faces on a TiB_2 particle of the kind in Al–Ti–B inoculants) or of a sphere. The case of octahedral TiC particles (of the kind in Al–Ti–C inoculants) has also been considered. When the nucleant surface is planar, a thin layer of solid formed on it can thicken to a metastable equilibrium configuration in which its interface with the liquid has a curvature equal to that of a critical nucleus. The existence of this solid has a negligible effect on the form of latent heat release while it remains dormant, but it does provide the basis for athermal nucleation of a grain as the critical nucleus size decreases on cooling and the energy barrier for free growth disappears. In principle, thermal nucleation over an energy barrier could occur before the onset of free growth, but only for particles of the order of 1 nm in radius. Since the particles active in grain refinement have radii of the order of 1 μm, the possibility of thermal activation is negligible. Indeed, for particles large enough to be effective grain-refining nucleants (i.e. stifling columnar growth), thermal nucleation must always be negligible. What remains is athermal nucleation, which is deterministic giving a number of grains dependent on undercooling but not on time. In cases such as inoculation by potent nucleants, the classical analysis of stochastic heterogeneous nucleation cannot apply. Such cases are not restricted to the grain refinement of alloys, but include for example the action of ice-nucleating agents in living systems.

Acknowledgement

The second author is supported by an EPSRC CASE studentship associated with Alcan Inc.

References

[1] D.M. Stefanescu, G. Upadhya and D. Bandyopadhyay, Metall. Trans. A **21A** 997 (1990).
[2] M. Rappaz and Ch.-A. Gandin, Acta Metall. Mater. **41** 345 (1993).
[3] Ph. Thévoz, J.L. Desbiolles and M. Rappaz, Metall. Trans. A **20A** 311 (1989).
[4] J.C. Fisher, J.H. Hollomon and D. Turnbull, J. Appl. Phys. **19** 775 (1948).
[5] T.E. Quested and A.L. Greer, Acta Mater. **53** 2683 (2005).
[6] D. Turnbull, J. Chem. Phys. **20** 411 (1952).
[7] D. Turnbull, Acta Metall. **1** 8 (1953).
[8] P. Schumacher, A.L. Greer, J. Worth, *et al*., Mater. Sci. Technol. **14** 394 (1998).
[9] A.L. Greer, A.M. Bunn, A. Tronche, *et al*., Acta Mater. **48** 2823 (2000).
[10] I. Maxwell and A. Hellawell, Acta Metall. **23** 229 (1975).
[11] N.H. Fletcher, J. Chem. Phys. **29** 572 (1958).
[12] N.H. Fletcher, J. Chem. Phys. **31** 1136 (1959).
[13] N.H. Fletcher, J. Chem. Phys. **38** 237 (1963).
[14] D.G. McCartney, Int. Mater. Rev. **34** 247 (1989).
[15] B.S. Murty, S.A. Kori and M. Chakraborty, Int. Mater. Rev. **47** 3 (2002).
[16] A.L. Greer, P.S. Cooper, M.W. Meredith, *et al*., Adv. Eng. Mater. **5** 81 (2003).
[17] T.E. Quested, Mater. Sci. Technol. **20** 1357 (2004).
[18] G.P. Jones, in *Solidification Technology in the Foundry and Cast House* (The Metals Society, London, 1983), pp. 112–114.
[19] G.P. Jones, in *Solidification Processing 1987*, edited by J. Beech and H. Jones (The Institute of Metals, London, 1988), pp. 496–499.
[20] J.W. Christian, *The Theory of Transformations in Metals and Alloys*, 2nd ed. (Pergamon, Oxford, 1975), pp. 418–475.
[21] N. Eustathopoulos, L. Coudurier, J.C. Joud and P. Desré, J. Cryst. Growth **33** 105 (1976).
[22] T.E. Quested and A.L. Greer, Acta Mater. **52** 3859 (2004).
[23] T.E. Quested, A.T. Dinsdale and A.L. Greer, Acta Mater. **53** 1323 (2005).
[24] D. Turnbull, J. Chem. Phys. **18** 198 (1950).
[25] W. Schneider, M.A. Kearns, M.J. McGarry, *et al*., in *Light Metals 1998*, edited by B. Welch (TMS, Warrendale, PA, 1998), pp. 953–961.
[26] A.L. Greer and A. Tronche, in *Continuous Casting*, edited by K. Ehrke and W. Schneider (DGM and Wiley-VCH, Weinheim, Germany, 2000), pp. 149–153.
[27] A. Tronche and A.L. Greer, Phil. Mag. Lett. **81** 321 (2001).
[28] S.F. Jones, G.M. Evans and K.P. Galvin, Adv. Colloid Interface Sci. **80** 27 (1999).
[29] G. Liger-Belair, M. Vignes-Adler, C. Voisin, *et al*., Langmuir **18** 1294 (2002).
[30] G. Liger-Belair, Sci. Am. **288**(1) 68 (January 2003).
[31] K.E. Zachariassen and E. Kristiansen, Cryobiology **41** 257 (2000).
[32] A.G. Govidarajan and S.E. Lindow, Proc. Natl. Acad. Sci. USA **85** 1334 (1988).
[33] M.J. Burke and S.E. Lindow, Cryobiology **27** 80 (1990).